Tellus (2008), 60B, 416–431
Printed in Singapore. All rights reserved

TELLUS

Surfactant partitioning in cloud droplet activation: a study of C8, C10, C12 and C14 normal fatty acid sodium salts

By NØNNE L. PRISLE[1], TOMI RAATIKAINEN[2], RIIKKA SORJAMAA[3], BIRGITTA SVENNINGSSON[1], ARI LAAKSONEN[2,3] and MERETE BILDE[1]*, [1]*Department of Chemistry, University of Copenhagen, Universitetsparken 5, DK-2100 Copenhagen, Denmark;* [2]*Finnish Meteorological Institute, Erik Palmenin Aukio 1, FI-00101 Helsinki, Finland;* [3]*Department of Physics, University of Kuopio, POB 1627, FI-70211 Kuopio, Finland*

(Manuscript received 25 October 2007; in final form 3 March 2008)

ABSTRACT

We have measured critical supersaturations of dried single-component particles of sodium caprylate [$CH_3(CH_2)_6COONa$], sodium caprate [$CH_3(CH_2)_8COONa$], sodium laurate [$CH_3(CH_2)_{10}COONa$] and sodium myristate [$CH_3(CH_2)_{12}COONa$] in the diameter range 33–140 nm at 296 K using a static thermal gradient diffusion cloud condensation nucleus counter. These fatty acid sodium salts are surface active molecules which have all been identified in atmospheric aerosol particles. Experimental critical supersaturations increased systematically with increasing carbon chain length and were in the range 0.96–1.34% for particles with a dry diameter of 40 nm. The experimental data were modelled using Köhler theory modified to account for partitioning of the surface active fatty acid sodium salts between the droplet bulk and surface as well as Köhler theory including surface tension reduction without accounting for surfactant partitioning and Köhler theory using the surface tension of pure water. It was found that Köhler theory using the reduced surface tension with no account for surfactant partitioning underpredicts experimental critical supersaturations significantly, whereas Köhler theory modified to account for surfactant partitioning and Köhler theory using the surface tension of pure water reproduced the experimental data well.

1. Introduction

This work is focused on understanding the role of surface active molecules in cloud droplet formation. In particular, we have studied the cloud droplet activation of a series of fatty acid sodium salts.

Fatty acids and their salts are found in aerosol particles over oceans as well as in urban and continental background locations. Over oceans, their concentrations typically range from below 1 to 30 ng m^{-3} (Gagosian et al., 1981, 1987; Mochida et al., 2002, 2003a,b, 2007), while at urban locations the concentrations of fatty acids can reach several $\mu g\, m^{-3}$ (Yassaa et al., 2001; Li and Yu, 2005). At background continental sites, intermediate concentrations are found (Graham et al., 2003; Cheng et al., 2004).

The low molecular weight fatty acids found at remote marine locations are thought to have mainly marine sources, although it has been shown that lipids are transported from terrestrial sources to the oceans (Gagosian et al., 1981, 1987). O'Dowd et al. (2004) showed that the concentration of organic material in marine air is higher during periods of high biological activity in the oceans, compared to low activity periods. Blanchard (1964) also demonstrated that the amount of surface active compounds in the aerosol correlates with the amount of sea salt. Particles enriched in organic compounds, compared to the bulk sea water, are produced by bubble bursting, where compounds found in the sea–air surface film and those scavenged by the ascending droplets are injected to the air.

Due to sea water pH, fatty acids in the ocean will mainly exist in the ionic form (Tabazadeh, 2005). In the marine aerosol, a major fraction of the fatty acids exists as sodium salts (Gagosian et al., 1981, 1987). Also in the eastern Mediterranean region, a major fraction of the fatty acids exists as salts (Stephanou, 1992).

*Corresponding author.
e-mail: mbilde@kemi.ku.dk
DOI: 10.1111/j.1600-0889.2008.00352.x

In sea salt aerosol containing fatty acids, loss of hydrochloric acid and formation of sodium salts of the fatty acids can be expected.

Mochida et al. (2002) report a positive correlation between low molecular weight (C_{14}–C_{19}) fatty acids and sea salt, with average fatty acid-to-sea salt mass ratios of 3×10^{-4}. Nevertheless, these fatty acids are among the most abundant of the identified organic compounds in the marine aerosol. Their concentration in individual submicrometre particles can also be much higher since they show a concentration maximum in the submicrometre particle range (Mochida et al., 2007), while the supermicrometre sizes dominate for sea salt mass. The submicrometre sea salt particles are, however, important number-wise and will thus be important for cloud droplet formation.

The salts of fatty acids with even carbon numbers show higher concentrations compared to those with odd carbon numbers, in accordance with biogenic emissions (Gagosian et al., 1981, 1987; Gogou et al., 1994; Mochida et al., 2002, 2007). A similar pattern is seen also for fatty acids at continental sites (Yassaa et al., 2001; Graham et al., 2003; Cheng et al., 2004; Li and Yu, 2005; Yassaa and Cecinato, 2005).

Sodium salts of fatty acids are surface active, which means that they concentrate on air–water surfaces. This can affect several atmospheric processes. The effect of interest in this work is the influence of surface activity on the reduction of surface tension as well as water activity in solution droplets compared to pure water and thereby facilitation of cloud droplet formation. The inability of the scientific community to assess the effect of aerosols on cloud formation with high confidence contributes to the most pronounced uncertainty in the global radiation balance (IPCC, 2007).

It has been demonstrated that bulk samples of atmospheric cloud/fog water and dissolved aerosol particles have lower surface tension compared to pure water (Gill et al., 1983; Seidl and Hanel, 1983; Facchini et al., 2000; Latif and Brimblecombe, 2004; Kiss et al., 2005).

It is, however, still unclear how to correctly apply the surface tension data to small droplets with high surface-to-volume ratios. A research effort combining detailed modelling and experiments has therefore been undertaken within the BACCI Nordic Centre of Excellence with the aim of correctly describing cloud droplet activation of atmospheric aerosols containing surface active molecules and to assess the effect of surfactant partitioning. It has been shown that Köhler theory using reduced surface tension, but ignoring partitioning of the surfactant molecules may significantly underestimate the critical supersaturation of particles comprising the model compound sodium dodecyl sulfate (Sorjamaa et al., 2004). This effect was also described in part by Li et al. (1998).

In the present work, we have studied the effect of surfactant partitioning for particles of pure sodium salts of normal fatty acids, a group of compounds with high atmospheric relevance. We present experimental data as well as model results for cloud droplet activation of aerosol particles of sodium caprylate, sodium caprate, sodium laurate and sodium myristate, respectively.

2. Experimental

We have measured the critical supersaturation as a function of dry particle diameter for single-component aerosol particles of the sodium salts of four straight-chain fatty acids: n-octanoic (caprylic), n-decanoic (capric), n-dodecanoic (lauric) and n-tetradecanoic (myristic) acid. The fatty acid sodium salts belong to a class of compounds comprising metallic salts of aliphatic carboxylic acids which are also called soaps. Chemicals were obtained from commercial sources: sodium caprylate (Sigma, capillary GC, minimum 99%), sodium caprate (Fluka, purum $\geq$ 98%), sodium laurate (Sigma, Sigma Grade 99–100%), sodium myristate (Sigma, Approx. 99%) and ammonium sulfate (Sigma-Aldrich, 99.999%). The organic salts are all solid at room temperature. Physical properties of the organic salts are given in Table 1. De-ionized water purified to a conductivity of 0.055 μS (corresponding to a resistivity of 18.2 MΩ cm) in a Milli-Q Plus Ultra Pure Water System was used for making aqueous

Table 1. Properties of the four fatty acid sodium salts used in model calculations

	Sodium caprylate	Sodium caprate	Sodium laurate	Sodium myristate
Formula	$CH_3(CH_2)_6COONa$	$CH_3(CH_2)_8COONa$	$CH_3(CH_2)_{10}COONa$	$CH_3(CH_2)_{12}COONa$
M (kg mol^{-1})	0.166	0.194	0.222	0.250
ρ (kg m^{-3})	1000[a]	1000[a]	1000[a]	1000[a]
Surface tension parameterization a (N m^{-1} K^{-1}), b	$a = 1.975 \times 10^{-4}$, $b = 363.2$	$a = 1.958 \times 10^{-4}$, $b = 1437$	$a = 1.707 \times 10^{-4}$, $b = 1.740 \times 10^4$	$a = 6.502 \times 10^{-5}$, $b = 4.713 \times 10^5$
cmc (mM)	351[b]	95.5[b]	23[b]	6.9[b]
ν_o	2	2	2	2

[a]Estimated.

[b]Campbell and Lakshminarayanan (1965).

Table 2. Experimental conditions

Compound and date of experiment	D_p (nm), dried particle diameter	RH (%)	CN (cm^{-3})	Q_{sample}/Q_{sheath}
Sodium caprylate				
21 March 2007	33, 35, 37, 40, 45, 50, 65, 85, 120	8.8–28	330–595	0.09–0.10
24 March 2007	34, 38, 42, 55, 75, 100	6.8–8.8	210–790	0.09–0.10
25 March 2007	34, 40, 50, 85	NaN	400–870	0.09–0.10
24 April 2007	35, 45	4.2	680–1320	0.12
Sodium caprate				
10 March 2007	35, 40, 45, 50, 60, 70, 85, 100, 135	NaN	310–650	0.09–0.10
13 March 2007	37, 55, 80 120	NaN	420–780	0.09–0.10
24 April 2007	36, 46	4.6	520–815	0.12
Sodium laurate				
25 January 2007	60, 80, 100, 120	4.8–9.8	410–570	0.09
29 January 2007	35, 37, 40, 45, 50, 60, 80, 120	17–24	407–890	0.08–0.09
02 February 2007	35, 40, 50, 80	8.6	380–780	0.08–0.10
24 April 2007	37, 47	4.6	550–940	0.12
Sodium myristate				
26 March 2007	42, 45, 48, 53, 60, 70, 85, 105, 140	47	330–720	0.09–0.10
27 March 2007	40, 41, 43, 50, 65, 75, 90, 120	24	220–810	0.10
25 April 2007	38, 48	4.5	465–540	0.12

solutions of the individual salts. Total concentrations were in the range 0.15–0.40 g L^{-1}.

For the longer carbon chain organic salts, it was in some cases necessary to stir solutions prior to the experiments for half an hour to dissolve the salt. In case of sodium myristate, solutions were in addition heated gently for 10 min and a fine suspension of the solute remained visible in the bottle. Purified and dried high-pressure air was used in all experiments.

The experimental set-up used in this work is similar to the system shown in fig. 2a of Henning et al. (2005) and will only be described briefly here. Particles were produced by atomizing aqueous solutions of the individual salts using a constant output atomizer (TSI-3076) operated in recirculation mode. The particles were subsequently dried by passing through a set of two silica gel containing diffusion driers in series. The resulting polydisperse aerosol was neutralized using a bipolar Kr-85 charger (TSI-3012). After further drying of the aerosol by dilution with dry air, a narrow electrical mobility particle size fraction was selected with an electrostatic classifier (TSI-3080) comprising an additional Kr-85 bipolar charger (TSI-3077) and a differential mobility analyser (DMA, TSI-3081). The sample-to-sheath air flow ratio (Q_{sample}/Q_{sheath}) in the DMA was in the range 0.08–0.10, except for a few test experiments with a ratio of 0.12. Particle electrical mobility diameters (D_p) selected for the experiments were in the range 33–140 nm. The relative humidity (RH) in the aerosol flow was measured immediately before the DMA using a dew point monitor (General Eastern Hygro-M4, dew point accuracy ±0.2 K) and was varied between 4 and 28%, with one exception of 47% (see also Table 2).

Critical supersaturations were measured with a static thermal gradient diffusion type cloud condensation nucleus counter, Wyoming CCNC-100B (Delene and Deshler, 2000; Snider et al., 2006). Particles entering the diffusion chamber are exposed to a controlled supersaturation in the range 0.2–2.0% and the number concentration of activated particles (CCN) at a given supersaturation is detected via light scattering. The total particle number concentration (CN) was measured in parallel using a condensation particle counter (TSI-3010).

An example of the experimental data obtained for dried sodium laurate particles with a diameter of 60 nm is shown in Fig. 1. The figure shows the fraction of activated particles (CCN/CN) as a function of the supersaturation the particles were exposed to. Each point in the figure represents one filling of the CCN-counter. As seen from the figure, activation occurs in two steps. We ascribe the first step to the activation of larger double-charged particles. The data were fitted using a four-parameter sigmoidal function, $y = y_0 + a/\{1 + \exp[-(x - x_0)/b]\}$. Correction for double-charged particles was achieved by fixing the fourth parameter (y_0) of the sigmoidal function to the fraction of double charged particles, identified by a visual inspection of the data. The critical supersaturation for the single-charged particles then was determined as the point of 50% of the remaining activation step (x_0).

The supersaturation in the CCN-counter was calibrated as described in Bilde and Svenningsson (2004) using monodisperse ammonium sulfate particles. It is assumed that traditional Köhler theory is valid for these particles. No particle shape factor was applied and the water activity was parameterized as a function of droplet concentration according to Low (1969). A linear

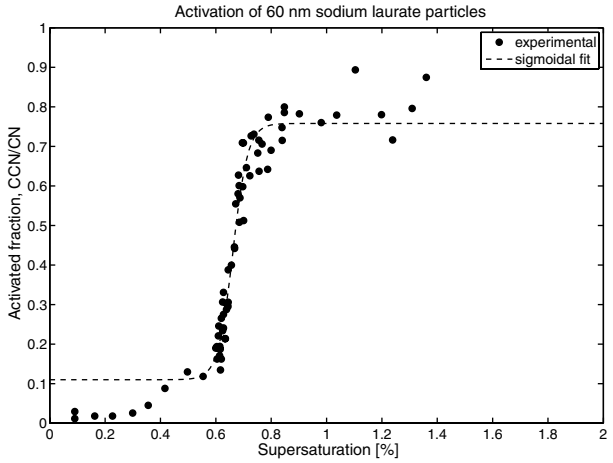

Fig. 1. Activated fraction of sodium laurate particles versus supersaturation in the CCN-counter. The diameter of the dry particles was 60 nm.

relation between the theoretical (Köhler theory) and measured critical supersaturations was obtained, SS_c (measured,%) = 1.4882 SS_c (theoretical,%) − 0.0287, and used to correct all experimental data.

All experiments were performed at room temperature. Temperatures were kept constant during the course of each experiment by the thermostat air condition system in the laboratory and were in the range 296 ± 2 K. The residence time in the tubing between the DMA and the CCN-counter was ∼0.2 s. To test for evaporation of particles in the tubing, the residence time was increased to ∼1.0 s by inserting additional tubing. This did not lead to any changes in the measured critical supersaturations. Further tests were performed by measuring the particle size after the DMA with a scanning mobility particle sizer (SMPS, TSI-3936) system. Based on these tests, we conclude that evaporation of the dried particles in the tubing between the DMA and the CCN-counter was insignificant. Table 2 shows the conditions for the experiments performed.

The error bars on the experimental critical supersaturations shown in this work reflect the 95% confidence intervals corresponding to $\pm 2\tau$, where τ is the combined standard deviation of the experimental critical supersaturation from the sigmoidal fit and the calibration equation for the supersaturation given above (Prisle, 2006).

3. Theory

Cloud droplet activation can be described by Köhler theory (Köhler, 1936) which gives a relation (the Köhler equation) between the equilibrium saturation ratio S of water vapour above an aqueous solution droplet and the droplet diameter d:

$$S = \frac{p_w}{p_w^0} = a_w \exp\left(\frac{4\nu_w \sigma}{RTd}\right), \quad (1)$$

where p_w is the equilibrium partial pressure of water over the solution droplet, p_w^0 is the equilibrium water vapour pressure over a flat surface of pure water, a_w is the droplet solution water activity, ν_w is the partial molar volume of water in solution, σ is the droplet solution surface tension, R is the universal gas constant and T is the Kelvin temperature. ν_w has been approximated by the molar volume of pure water, $\nu_w^0 = M_w/\rho_w$, where M_w and ρ_w are the molar mass and mass density of pure water, respectively. For convenience, we refer to the supersaturation, defined as $SS = S - 1$. The critical supersaturation SS_c is the maximum of a plot of equilibrium supersaturation versus droplet diameter, the so-called Köhler curve. Particles that have been exposed to supersaturations larger than their critical supersaturation and grown beyond the corresponding critical droplet diameter d_c are activated to cloud droplets and continue to grow limited only by the transport of water to the droplet surface.

The first term in the Köhler equation (a_w) is called the Raoult term and accounts for the decrease in the water partial pressure over the droplet due to dissolved solutes. The exponential term accounts for the increase in water vapour pressure due to the droplet curvature and is called the Kelvin term. The magnitude of this increase depends directly on the droplet solution surface tension (σ).

Surface active compounds, or surfactants, decrease the surface tension of aqueous solutions from the pure water value. The surfactants studied in this work belong to a class of organic molecules or ions with polar head-groups and non-polar hydrocarbon tails. In aqueous solutions, these surfactants preferentially concentrate in the solution surface with the hydrocarbon tails pointing out towards the air to minimize unfavourable interactions with water. We refer to this as surfactant partitioning. In macroscopic solutions, surfactant partitioning to the solution surface further enhances the surface tension reduction due to the surfactant.

The partitioning of surfactant molecules between the solution surface and bulk depends on both the nature of the surfactant and the dimensions of the solution system. Microscopic droplets have a much larger surface area-to-bulk volume ratio than macroscopic bulk solutions. Therefore, for the same total number of surfactant molecules per unit volume of water, a larger fraction of the surfactant molecules will reside in the surface of a microscopic droplet compared to the surface of a macroscopic bulk solution. The droplet bulk is thus depleted in the surfactant and when the partitioning equilibrium is established the surfactant concentrations will consequently be smaller in both the surface (molecules per unit area) and bulk (molecules per unit volume) of microscopic droplets compared to macroscopic bulk solutions. This is illustrated in Fig. 2.

The consequences of surfactant partitioning for cloud droplet activation are twofold. Since the resulting surfactant concentration in the surface is smaller for microscopic droplets than for macroscopic bulk solutions, the surface tension is not reduced as much in the microscopic droplet as in the macroscopic bulk

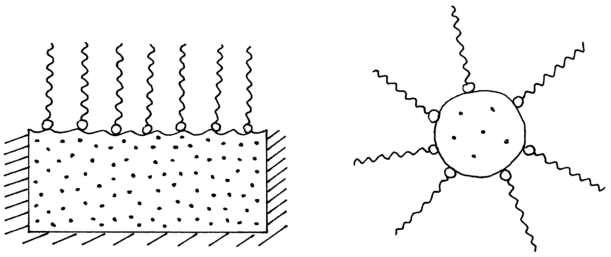

Fig. 2. Schematic drawing illustrating surfactant partitioning in a macroscopic bulk solution (left-hand panel) and in a microscopic droplet (right-hand panel). Partitioning results in smaller surfactant concentrations in both the surface (molecules per unit area) and the bulk (molecules per unit volume) of the microscopic droplet compared to the macroscopic bulk solution.

solution for a given total surfactant concentration. This leads to a smaller decrease in equilibrium water vapour pressure over the microscopic droplet from the surface tension reduction in the Kelvin effect than if the surface tension of the corresponding macroscopic bulk solution with the same total surfactant concentration were applied. This was addressed by Li et al. (1998). Furthermore, as the bulk of a microscopic droplet is comparatively more depleted in the surfactant molecules due to partitioning to the surface, a given total concentration of surfactant solute yields a smaller water partial pressure reduction, or Raoult effect, than in a macroscopic bulk solution. Both these effects of surfactant partitioning thus act to increase the equilibrium water vapour pressure over microscopic droplets compared to that predicted using the total surfactant concentration and surface tension properties of corresponding macroscopic bulk solutions. This was taken into account in the model of Sorjamaa et al. (2004) and the same approach was used in this work.

4. Model

The cloud droplet activation of the four fatty acid sodium salts has been modelled using three different approaches based on Köhler theory as described above: (1) accounting for surfactant partitioning following Sorjamaa et al. (2004) (referred to as 'partitioning' in the following), (2) disregarding surfactant partitioning and evaluating both water activity and surface tension of the droplet assuming that all surfactant molecules are present in the bulk (referred to as 'bulk σ') and (3) disregarding both partitioning and surface tension reduction by the surfactant, that is, assuming the surface tension of pure water for the droplet solution and evaluating the water activity with all surfactant molecules in the droplet bulk (referred to as 'σ_{w}').

Below we focus on describing the 'partitioning' modelling approach based on Sorjamaa et al. (2004). We also provide information about the surface tension parameterizations, water solubilities and particle densities used and discuss briefly surfactant micelle formation, sodium counterion binding and carboxylate ion protonation.

4.1. The partitioning modelling approach

The partitioning model has been described in detail by Sorjamaa et al. (2004), so only a brief overview is given here. Bulk concentrations in the partitioning model are calculated from the Gibbs adsorption equation (Gibbs et al., 1928). In the case of a single ideal solute, the adsorption equation simplifies to:

$$n_{\mathrm{w}}^{\mathrm{T}} RT\,\partial \ln\left(1 - x_{\mathrm{o}}^{\mathrm{B}}\right) + \nu_{\mathrm{o}} n_{\mathrm{o}}^{\mathrm{T}} RT\,\partial \ln\left(x_{\mathrm{o}}^{\mathrm{B}}\right) + A\partial\sigma = 0, \qquad (2)$$

where A is the droplet surface area, ν_{o} is the dissociation factor for the organic salt and n_i^{T} and x_i^{B} are the total number concentration and droplet bulk phase mole fraction for species i, respectively. Mole fractions were used instead of activities, corresponding to assuming ideality of the droplet bulk phase, as activity coefficient data were unavailable. The surface tension gradient is calculated using surfactant bulk mole fractions ($x_{\mathrm{o}}^{\mathrm{B}}$). The total water number concentration ($n_{\mathrm{w}}^{\mathrm{T}}$) is calculated from the volume of water in the droplet, determined as the difference between droplet and dry particle volumes ($V_{\mathrm{w}} = V_{\mathrm{droplet}} - V_{\mathrm{particle}}$), using the molar volume of pure water ($n_{\mathrm{w}}^{\mathrm{T}} = V_{\mathrm{w}}/\nu_{\mathrm{w}}^{0}$).

Surfactant partitioning has been modelled assuming electroneutrality of the droplet bulk and surface phases, such that equal amounts of carboxylate anions and sodium cations partition to the surface regardless of the dissociation state in the bulk. In the model description, the surface phase contains both the topmost layer dominated by carboxylate anions and subsurface layers, where sodium cations have enhanced concentrations. The net charge of these layers comprising the surface phase is zero.

4.2. Surface tension parameterization

Model calculations employ equilibrium surface tensions of the growing droplets. The equilibrium surface tension at a given solution concentration decreases systematically with carbon chain length from sodium caprylate to sodium myristate, but the values reported vary considerably (Campbell and Lakshminarayanan, 1965; Van den Bogaert and Joos, 1979, 1980; Wen et al., 1998; Fainerman et al., 2002; Luepakdeesakoon et al., 2006). This may be due to both dynamic effects such as measurement time scales and to the actual method of surface tension measurement (Coltharp and Franses, 1996; Wen et al., 1998). Very different equilibration times are reported in the literature for the studied fatty acid sodium salts, for sodium myristate from the order of 1 s (Van den Bogaert and Joos, 1979, 1980) to the order of 10^3 s (Wen et al., 1998).

The size of the growing droplets in the CCN-counter is several orders of magnitude smaller than the bulk systems for which surface tension has been measured (μm compared to mm), as for example by Campbell and Lakshminarayanan (1965). A crude calculation assuming that the diffusion time of sodium myristate to the surface is proportional to the distance accordingly gives equilibrium times of the order of 1 s (or less) in the microscopic droplets. The surfactant molecules should thus have enough time

to diffuse to the surface within the time frame of a CCN measurement (20 s), even if the macroscopic equilibration times are rather long. Furthermore, Taraniuk et al. (2007) found that the diffusion of humic-like substances (HULIS) to the surface of growing droplets is faster than the time scale of droplet growth under typical tropospheric conditions. The molecular masses of the fatty acid salts span the range 166–250 Da. This is smaller than or comparable to the average molecular mass of atmospheric HULIS which was found to be in the 200–345 Da (Kiss et al., 2003) or 200–500 Da (Emmenegger et al., 2007) range. It therefore seems reasonable to use equilibrium surface tensions in the cloud droplet activation model calculations in this work.

In the model calculations, a parameterization of the equilibrium surface tension as a function of bulk concentration of surfactant molecules is applied during droplet growth and activation. Measurements of equilibrium surface tensions as a function of surfactant concentration in aqueous macroscopic bulk solutions at 298 K were obtained for all four fatty acid sodium salts from Campbell and Lakshminarayanan (1965). Surfactants form micelles in concentrated solutions above the so-called critical micelle concentration (cmc). Parameterizations were obtained by fitting the surface tension data below the critical micelle concentrations with the Szyskowski equation (Szyskowski, 1908):

$$\sigma = \sigma_{\mathrm{w}} - aT \log_{10}\left[1 + b \min(x_{\mathrm{o}}, x_{\mathrm{o}}^{\mathrm{cmc}})\right], \tag{3}$$

where σ_{w} ($\mathrm{N\,m^{-1}}$) is the surface tension of pure water, a ($\mathrm{N\,m^{-1}\,K^{-1}}$) and b are the fitting parameters, T (K) is the temperature, x_{o} is the organic surfactant mole fraction in solution and $x_{\mathrm{o}}^{\mathrm{cmc}}$ is the critical micelle concentration given as organic surfactant mole fraction. Both mole fractions denote undissociated surfactant. The surface tension parameterization is therefore independent of the actual dissociation state of the fatty acid salts in solution. Parameters obtained from the Szyskowski fits are given in Table 1.

In the beginning of droplet growth, the droplets are concentrated solutions of the surfactant solute above the critical micelle concentration. Above the cmc, it is assumed that the droplet solution surface tension is constant. As the droplet grows it becomes increasingly dilute and when the surfactant bulk mole fraction reaches below the cmc, the surface tension gradient (with respect to increasing surfactant bulk mole fraction) changes discontinuously from zero to a large negative value. At this point, the modelling of partitioning by the adsorption equation (eq. 2) therefore starts.

The constant droplet solution surface tension at surfactant bulk concentrations above the cmc could be interpreted such that the bulk concentration of unassociated surfactant is constant (and equal to the cmc) and any remaining surfactant is distributed between residing in the droplet surface and forming micelles in the droplet bulk. However, the surfactant water solubility will always be greater than the cmc and if the bulk concentration of unassociated surfactant is limited to the value of the cmc, there will be a gap in the modelled surfactant bulk concentration, from the solubility limit to the cmc. To avoid this problem, the actual formation of micelles is ignored in the model and all associated surfactant molecules are considered as individual species in the droplet bulk phase. The surfactant surface excess (Γ, molecules per unit surface area) is assumed to be constant for droplets above the cmc and equal to the maximum value (Γ^{max}) found at surfactant bulk concentrations equal to the cmc. The total number of surfactant molecules in the droplet surface above cmc is then determined by scaling the maximum surface excess value to the droplet surface area.

Now, the surfactant bulk mole fraction and surface excess as well as the droplet solution surface tension are continuous functions of the droplet diameter. When the surfactant bulk mole fraction exceeds the cmc, both surfactant surface excess and droplet solution surface tension are constants.

The above assumptions of constant surfactant surface excess and ignoring micelles in the droplet above the cmc are both non-standard approximations but necessary in order to model the full range of droplet growth and activation. These approximations rarely have an effect on the predicted critical supersaturations, because activation occurs at larger droplet sizes where the droplets are diluted below the cmc and the assumptions thus no longer apply. Model calculations have been performed taking the limited water solubility of the surfactant into account. When governed by the surfactant solubility limit, activation occurs with the onset of deliquescence and the surfactant solute concentration in the droplet bulk is equal to the water solubility and therefore still independent of the given approximations.

Different approximations to the droplet solution properties above the surfactant cmc could produce different modelling results. For example, the surfactant bulk concentration could be limited to the cmc with the remaining surfactant ions in the droplet bulk forming micelles, which may be assumed to have negligible influence on the total bulk concentration of dissolved species. If the cmc is sufficiently small, the predicted critical supersaturations would then be higher, by the same principle as when surfactant water solubility limits the droplet bulk concentration.

4.3. Water solubility

Water solubilities for sodium caprylate and sodium myristate have been reported as approximately 0.5 $\mathrm{kg\,kg^{-1}}$ (Kertes et al., 1985) and 0.002 $\mathrm{kg\,kg^{-1}}$ (Wen and Franses, 2000), respectively. To the best of our knowledge, no literature values are available for the corresponding water solubilities of sodium caprate and sodium laurate. Instead, we therefore used the largest concentrations reported by Campbell and Lakshminarayanan (1965) as solubility limits for each of the fatty acid sodium salts studied. These limiting concentrations decrease in order of increasing carbon chain length as expected for the water solubilities of the fatty acid sodium salts (Wen et al., 1998) and the values for sodium caprylate and sodium myristate are comparable to the

water solubilities reported by Kertes et al. (1985) and Wen and Franses (2000).

4.4. Micelles, sodium counterion binding and carboxylate protonation

Surfactants are expected to form micelles in the growing droplets until the surfactant concentration in the droplet bulk reaches below the critical micelle concentration. Micelle formation decreases the bulk concentration of unassociated surfactant molecules and thus affects both water activity and surface tension of the solution. Critical micelle concentrations for the fatty acid sodium salts are given in Table 1.

The electrostatic fields of anionic surfactant micelles may result in some degree of sodium counterion binding (Wen and Franses, 2000), which will reduce the effective concentration of sodium ions in solution and thereby decrease the water activity reduction (Raoult effect) from sodium ions. Such effects of sodium counterion binding have not been included in the model calculations.

In addition to micelles, other associated structures may form in surfactant solutions: The organic anions of the fatty acid sodium salts are carboxylate ions that can protonate in aqueous solution and form the corresponding carboxylic acids (Wen and Franses, 2000; Wen et al., 2000). The fatty acids are considerably stronger surfactants than their carboxylate anions (Fainerman et al., 2002) and presence of the acid in solution will affect the surface tension (Wen et al., 2000). The acids are, however, also much less water soluble than the corresponding sodium carboxylate salts, with solubilities of 8×10^{-4}, 1.5×10^{-4}, 5.5×10^{-5} and 2×10^{-5} kg kg^{-1} for caprylic, capric, lauric and myristic acid, respectively (CRC, 2004–2005), and will therefore tend to precipitate from solution. Furthermore, the acids will form complexes with the carboxylate anions of various stoichiometry and degree of sodium counterion binding, which may also precipitate (Wen and Franses, 2000; Wen et al., 2000). Such association and precipitation processes will again decrease the effective bulk concentration of the surfactant and possibly the sodium counterion and thus affect both water activity and surface tension of the droplet solutions.

The fatty acids are weak: pK_a is 4.89 for caprylic acid (CRC, 2004–2005), 4.9 for capric acid (Stahl and Wermuth, 2002), 5.3 for lauric acid (Van Egmond et al., 1999) and approximately 5.8 for myristic acid (Wen and Franses, 2000). We have not considered the various effects of carboxylate ion protonation explicitly in the model calculations, since droplet solutions at activation are predicted to be rather dilute (<0.1 M for the 'partitioning' approach and <0.5 M for the 'σ_w' approach, all dry particle sizes and compositions considered) and the protonation equilibrium therefore is shifted greatly in favour of the carboxylate ion form (e.g. $[CH_3(CH_2)_{12}COOH]/[CH_3(CH_2)_{12}COO^-] \ll 1$ for an initial sodium myristate concentration of 0.5 M). Even so, as the droplet surface tension has been parameterized as a function of surfactant bulk concentration from experimental data, the effect on surface tension and thus the Kelvin term is to some extent implicitly accounted for by the obtained parameterizations. Any effects in the Raoult term are, however, not accounted for.

4.5. Particle densities

To the best of our knowledge, no data on the mass densities of neither sodium caprylate, sodium caprate, sodium laurate or sodium myristate are available in the literature. The densities of the corresponding fatty acids are 907.3, 885.8, 867.9 and 862.2 kg m^{-3} for the C8, C10, C12 and C14 carboxylic acids, respectively (CRC, 2004–2005). We expect the densities of the salts to be higher than the densities of the corresponding acids and in all model calculations discussed herein we have estimated the densities of all four fatty acid salts to be 1000 kg m^{-3}. For comparison, the density of oleic acid ($CH_3(CH_2)_7CH = CH(CH_2)_7COOH$) is 893.5 kg m^{-3} (CRC, 2004–2005) and the density of the corresponding salt, sodium oleate, is 1096 kg m^{-3} (Ross and McBain, 1946).

4.6. Activity coefficients and dissociation

Literature activity coefficients for the fatty acid sodium salts are to our knowledge unavailable; however, experimental data on concentration dependent osmotic behavior of aqueous sodium laurate solutions have been reported and suggest that such solutions only deviate from ideal-dilute behaviour at concentrations above the sodium laurate cmc (Fineman and McBain, 1948). Critical supersaturations have been modelled assuming solution ideality for the growing droplets in terms of unity activity coefficients for all droplet constituents. The fatty acid sodium salts have been assumed to be either not dissociated or fully dissociated in the droplet bulk by applying dissociation factors $\nu_o = 1$ and 2, respectively.

5. Results and discussion

The four fatty acid sodium salts studied represent a homologous series of molecules where the carbon chain length increases in increments of two $–CH_2–$ groups. Figure 3 shows the measured critical supersaturations for all particle diameters of each of the four fatty acid sodium salts. It is clear that the critical supersaturation needed to activate the fatty acid sodium salts at a given particle diameter increases systematically with increasing carbon chain length. The same order of activation is reflected in the model results (not shown in this figure). For a particle with a diameter of 40 nm, the experimental critical supersaturation increases from 0.96% (average of two data points) for sodium caprylate (C8) to 1.10, 1.24 (average of two data points) and 1.34% for sodium caprate (C10), laurate (C12) and myristate (C14), respectively. For particles with a diameter of 100 nm, the corresponding experimental critical supersaturations are 0.27,

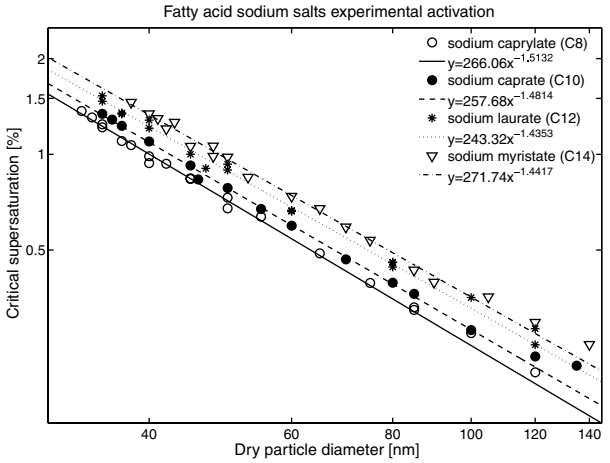

Fig. 3. Experimental critical supersaturations as a function of dry particle diameter for each of the carbon chain lengths. The lines are power functions fitted to the experimental data for each surfactant. See the text for details.

0.28 and 0.35% for sodium caprylate (C8), caprate (C10) and laurate (C12), respectively, and 0.36% for a 105 nm sodium myristate particle. In Fig. 3, the experimental data series for each of the fatty acid sodium salts have been fitted to a power function, $y = c \times x^b$. It is seen that the exponent in each case is close to the value of $b = -3/2$. This confirms the assumption of equilibrium with respect to diffusion of surfactants to the droplet surface: if equilibrium had not been reached, this effect would be more pronounced for the larger dry particle diameters than for the smaller ones and the power function exponent would deviate from the value of $b = -3/2$.

In Fig. 4a–d, measured critical supersaturations for sodium caprylate, sodium caprate, sodium laurate and sodium myristate particles are compared with the three modelling predictions previously mentioned: (1) accounting for surfactant partitioning following Sorjamaa et al. (2004) ('partitioning'), (2) disregarding surfactant partitioning and evaluating both droplet water activity and surface tension assuming that all surfactant molecules are present in the droplet bulk ('bulk σ') and (3) assuming a droplet surface tension equal to that of pure water and evaluating the water activity with all surfactant molecules in the droplet bulk ('σ_w'). The model results in Fig. 4a–d are shown for a dissociation factor $\upsilon_o = 2$ for each of the fatty acid sodium salts and full water solubility has been assumed in all cases. Representative Köhler curves calculated for initial particle diameters of 40 and 100 nm are shown as insets in each figure. The kink seen in some of the calculated Köhler curves appears when the droplet solution reaches the surfactant critical micelle concentration: As the droplet grows and the surfactant concentration decreases below the cmc, the droplet solution surface tension increases abruptly with droplet diameter from its constant value above the cmc. This change in droplet surface tension-to-droplet diameter ratio causes an abrupt change in the Kelvin term, which has a local minimum at the cmc. The droplet water activity given by the water mole fraction on the other hand changes smoothly at the cmc.

It is clear from the Fig. 4a–d that Köhler theory modified to account for surfactant partitioning as suggested by Sorjamaa et al. (2004) (approach 1) reproduces the experimental data well in all cases, whereas experimental critical supersaturations are significantly underpredicted if surface tension reduction by the surfactant is included and partitioning is not accounted for in neither the Kelvin nor the Raoult effect (approach 2).

Approach (3), where surfactant partitioning is ignored and the surface tension of pure water is used in the Kelvin term, also reproduces the data well.

To understand the similarity between the predictions of modelling approaches (1) and (3), we have calculated the surfactant bulk molar concentrations at activation for these two approaches, as well as the surfactant surface excess (molecules per unit area) at activation predicted by the partitioning approach (1). The surface excess only has meaning within the partitioning framework and was therefore not calculated when surfactant partitioning was ignored. Figure 5 shows the results for sodium caprate particles and similar results were obtained for each of the studied fatty acid sodium salts. Table 3 (a) gives predicted values for the critical droplet diameter (d_c), surfactant bulk concentration, water activity ($a_{w,c}$, assuming unity activity coefficients) and the Kelvin term ($S_{Kelvin,c}$) at activation along with the critical supersaturation calculated as $SS_c = (100\%) \times [(a_{w,c} \times S_{Kelvin,c}) - 1])$ for sodium caprate particles with initial sizes of 40 and 100 nm, respectively. Table 3(b) shows values of bulk surfactant concentration, water activity (a_w, assuming unity activity coefficients) and the Kelvin term (S_{Kelvin}) along with the equilibrium supersaturation calculated as $SS = (100\%) \times [(a_w \times S_{Kelvin} - 1)]$ for selected droplet diameters (d) during droplet growth, for the same initial particle diameters. Results are shown for all three model approaches: approach (1) accounting for surfactant partitioning, approach (2) including surface tension reduction without accounting for surfactant partitioning and approach (3) using the surface tension of pure water. It is seen from Table 3 and Fig. 5 that for the smaller particles, which activate at higher supersaturations and therefore form more concentrated droplets at the point of activation, the differences in surfactant bulk concentrations predicted by modelling approaches (1) and (3) are large and approach (1) predicts a significant surface excess of surfactant. Approach (3), which does not account for surfactant partitioning, accordingly predicts a significantly higher surfactant bulk concentration at activation than approach (1), which does take surfactant partitioning into account. The predicted Raoult effect is therefore larger in approach (3) than in approach (1) and, since the critical supersaturations and corresponding critical droplet diameters predicted by the two approaches are very similar, the greater Raoult effect in approach (3) is counteracted by the surface tension reduction by the surfactant included in approach (1).

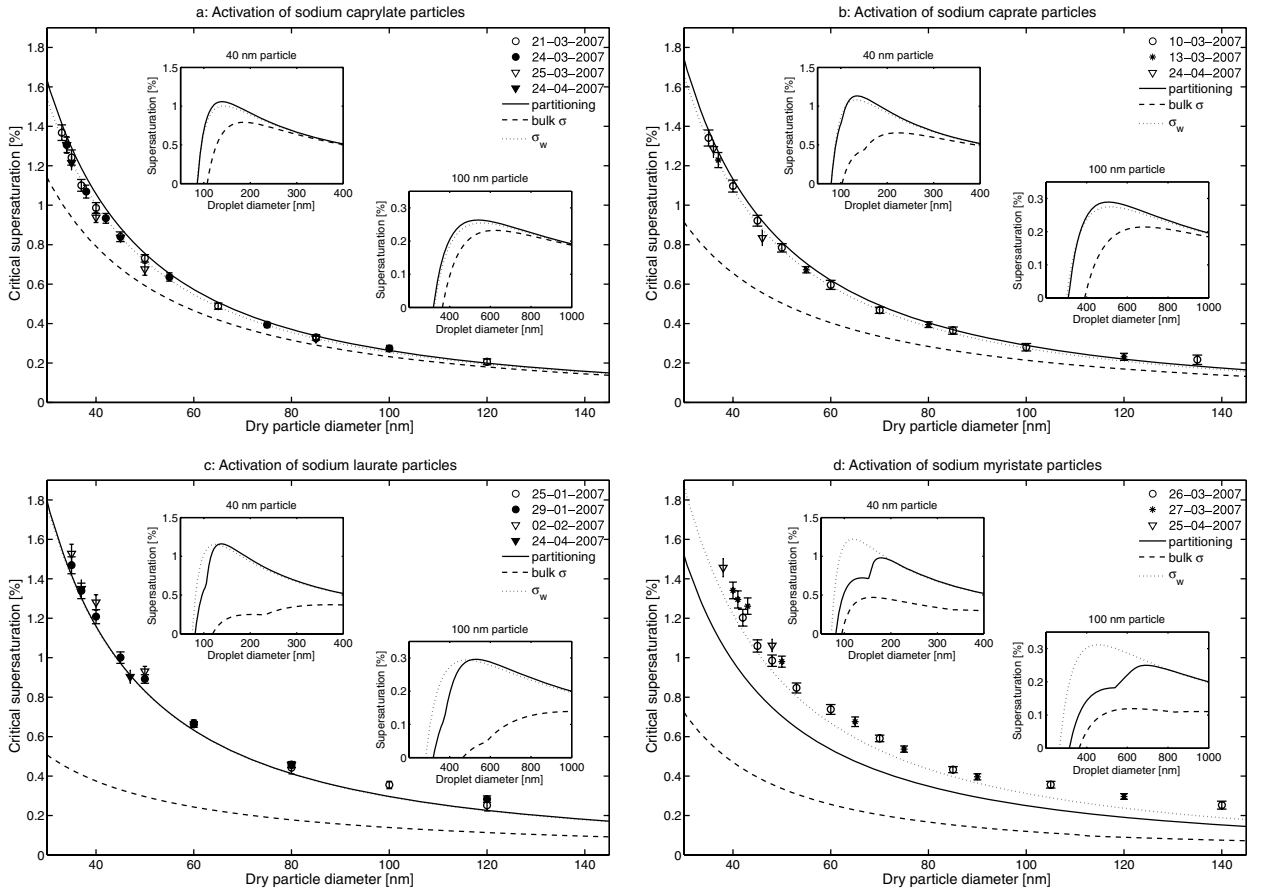

Fig. 4. Critical supersaturation as a function of dry particle diameter for (a) sodium caprylate, (b) sodium caprate, (c) sodium laurate and (d) sodium myristate. Experimental data are given in series according to the day of experiment. The lines represent the different modelling approaches: the full line labelled 'partitioning' accounts for surfactant partitioning. The dashed line labelled 'bulk σ' includes concentration-dependent surface tension during droplet growth but disregards partitioning of the surfactant. The dotted line labelled 'σ_w' does not consider surfactant partitioning and uses the constant surface tension of pure water. The insets show Köhler curves calculated by each modelling approach for initial dry particle diameters of 40 and 100 nm. Full water solubility and a dissociation factor of $\nu_o = 2$ for the organic salt was assumed in all cases. See the text for details.

The area of a laurate ion in a surface monolayer has been estimated to be 50 Å^2 = 5×10^{-19} m^2 (Shelley et al., 2000) and the other homologous fatty acid carboxylate ions studied can be expected to have comparable sizes in such monolayers. Modelling approach (1) predicts a surface excess at activation around 1–2 $\times 10^{18}$ molecules m^{-2} for the fatty acid sodium salts and particle diameters studied and thus the fractional droplet surface coverage by surfactant molecules is of the order of 0.5–1.0. We can therefore not draw the conclusion that cloud droplet activation of surface active species can in general be modelled using the constant surface tension of pure water and not accounting for surfactant partitioning. Instead, the agreement between critical supersaturations predicted by modelling approaches (1) and (3) suggests that when surfactant partitioning to the droplet surface is accounted for, the effects on the Kelvin and Raoult terms counteract one another: the water activity reduction by the surfactant solute is decreased as partitioning to the surface decreases the droplet bulk concentration. This is on the other hand balanced by the surface tension reduction by the surfactant, which decreases the Kelvin term, but not as much as if surfactant partitioning were not considered. Note that these considerations strictly apply for droplets of the same size and total surfactant concentration: for droplets of different diameters, the respective Raoult and Kelvin terms are not directly comparable from a point of surfactant partitioning, as the Raoult term will be affected by droplet dilution and the Kelvin term both by the influence of dilution on droplet surface tension and by the droplet curvature.

Droplets are generally predicted to be below critical micelle concentrations at activation for the partitioning approach (1), but the cmc may be exceeded at activation in the smaller droplets by modelling approach (3). The good agreement with experimental results observed for modelling approach (3) may thus be a coincidence of overpredicting the water activity reduction (Raoult effect) within this approach.

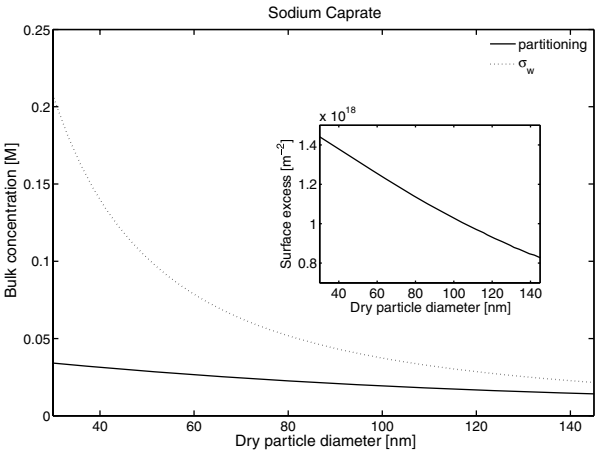

Fig. 5. Surfactant bulk molar concentrations at the point of activation as a function of dry particle diameter for sodium caprate particles, calculated from modelling approaches (1) ('partitioning') and (3) ('σ_w'). The inset shows surfactant surface excess at activation as a function of sodium caprate dry particle diameter, calculated from modelling approach (1) ('partitioning').

It is not necessarily the case that modelling approaches (1) (accounting for partitioning) and (3) (using the surface tension of pure water) will agree for other surfactants, as also demonstrated by Sorjamaa and Laaksonen (2006). Therefore, activation of particles containing different surfactants should be investigated further. As an example, using the constant surface tension of water and not accounting for surfactant partitioning overpredicts the experimental critical supersaturations for particles of sodium dodecyl sulfate and it is necessary to both employ reduced surface tension and account for surfactant partitioning to reproduce experimental data (Sorjamaa et al., 2004). We would also like to point out that for mixed particles including soluble components as, for example, inorganic salts in addition to surfactants, the balance between the Raoult and Kelvin terms may be altered (Li et al., 1998).

Another important point is that the droplet diameter at activation (d_c) predicted from approaches (2) and (3) can differ significantly from the value predicted when accounting for surfactant partitioning, that is, by approach (1). This is illustrated in Table 3(a) and in Fig. 4c. This may have important consequences in cloud modelling.

Cloud droplet activation of particles containing molecules with limited water solubility is more complicated than the activation of particles containing only fully soluble species. The Köhler equation must be modified to account for limited water solubility (Shulman et al., 1996; Kulmala et al., 1997; Laaksonen et al., 1998; Hori et al., 2003; Bilde and Svenningsson, 2004; Broekhuizen et al., 2004) resulting in a higher critical supersaturation than when full water solubility is assumed.

Cloud droplet activation was modelled for all three approaches assuming full water solubility as well as using the solubility limits mentioned in Section 4.3 for each of the fatty acid sodium salts studied. The activation of sodium caprylate and sodium caprate is not limited by water solubility, whereas the effect of limited solubility is seen for sodium laurate activation predicted by modelling approach (3). Solubility effects are also seen in modelling approach (2) for the smallest sodium laurate particle sizes. All modelling approaches predict a strong effect of limited water solubility on critical supersaturations for sodium myristate particles.

Sodium caprylate, sodium caprate and sodium laurate particles behaved in the experiments as though they were fully soluble and fully dissociated in the droplet bulk at activation. Sodium myristate particles activated at supersaturations much lower than predicted when accounting for limited water solubility, but still somewhat higher than predicted by the partitioning model using full solubility and full dissociation. Sodium myristate will be addressed separately below.

5.1. Sensitivity analysis

In the following, we will discuss the sensitivity of the partitioning model (approach 1) to surface tension parameterization, dry particle density (ρ), calculation of the partial molar volume of water in solution (ν_w), temperature (T), water and surfactant solute activity coefficients (γ_w and γ_o) and organic salt dissociation factor (ν_o). We will use sodium laurate as example molecule. Results of the sensitivity analysis are summarized in Table 4.

Several data sets of equilibrium surface tension measurements and parameterizations as a function of bulk solution concentration exist for the fatty acid sodium salts studied (Campbell and Lakshminarayanan, 1965; Van den Bogaert and Joos, 1980; Fainerman et al., 2002; Luepakdeesakoon et al., 2006; Kralchevsky et al., 2007). First, we tested the sensitivity of the model predicted critical supersaturations for sodium laurate particles to the application of a different equilibrium surface tension data set (Kralchevsky et al., 2007) with significantly lower equilibrium surface tensions and critical micelle concentration than that of Campbell and Lakshminarayanan (1965). Secondly, we tested the model sensitivity to a different surface tension parameterization equation (Hyvärinen et al., 2006):

$$\sigma = x_o\sigma_o + (1 - x_o)\sigma_w - RTx_o(1 - x_o)\left[\frac{c}{x_o + d(1 - x_o)} + \frac{e}{fx_o + 1 - x_o}\right], \quad (4)$$

where $\sigma_o = a + bT$ is the surface tension of the pure organic surfactant. Parameters a, b, c, d, e and f were fitted to both experimental surface tension data sets (Campbell and Lakshminarayanan, 1965; Kralchevsky et al., 2007) using data below the critical micelle concentrations and are given in the footnotes below Table 4.

Despite the differences in both equilibrium surface tension data and parameterization equations, the differences between predicted critical supersaturations are less than 4.5%.

Table 3: Calculations showing model predicted values for sodium caprate particles with initial sizes of 40 and 100 nm, respectively: Panel (a) shows the droplet diameter at activation (d_c) along with the corresponding surfactant bulk concentration, water activity ($a_{w,c}$, assuming unity activity coefficients), Kelvin term ($S_{Kelvin,c}$) and critical supersaturation calculated as $SS_c = (100\%) \times [(a_{w,c} \times S_{Kelvin,c}) - 1]$. Panel (b) shows the bulk surfactant concentration, water activity (a_w, assuming unity activity coefficients) and the Kelvin term (S_{Kelvin}) along with the equilibrium supersaturation calculated as $SS = (100\%) \times [(a_w \times S_{Kelvin}) - 1]$ for selected droplet diameters (d) during droplet growth. Results are shown for all three model approaches, (1) accounting for surfactant partitioning, (2) including surface tension reduction without accounting for surfactant partitioning and (3) using the surface tension of pure water, for both initial particle diameters

(a) Sodium caprate	d_c [nm]	Bulk concentration at activation [mM]	$a_{w,c}$ (Raoult term)	$S_{Kelvin,c}$ (Kelvin term)	SS_c [%]
Initial particle diameter: 40 nm					
Approach (1) "partitioning"	135.2	31	0.9989	1.0125	1.13
Approach (2) "bulk σ"	223.2	30	0.9989	1.0076	0.65
Approach (3) "σ_w"	133.1	140	0.9948	1.0161	1.08
Initial particle diameter: 100 nm					
Approach (1) "partitioning"	506.8	19	0.9993	1.0036	0.29
Approach (2) "bulk σ"	683.1	16	0.9994	1.0027	0.21
Approach (3) "σ_w"	516.5	37	0.9986	1.0041	0.27

(b) Sodium caprate	d [nm]	Bulk concentration [mM]	a_w (Raoult term)	S_{Kelvin} (Kelvin term)	SS [%]
Initial particle diameter: 40 nm					
Approach (1)	80	169	0.9937	1.0150	0.86
"partitioning"	120	49	0.9982	1.0127	1.09
	240	6	0.9998	1.0084	0.82
Approach (2)	80	644	0.9741	1.0150	−1.13
"bulk σ"	120	191	0.9929	1.0100	0.28
	240	24	0.9991	1.0074	0.65
Approach (3)	80	644	0.9741	1.0269	0.03
"σ_w"	120	191	0.9929	1.0178	1.06
	240	24	0.9991	1.0089	0.80
Initial particle diameter: 100 nm					
Approach (1)	300	109	0.9960	1.0040	0.00
"partitioning"	500	20	0.9993	1.0036	0.29
	700	8	0.9997	1.0028	0.26
Approach (2)	300	191	0.9929	1.0040	−0.32
"bulk σ"	500	41	0.9985	1.0032	0.17
	700	15	0.9995	1.0027	0.21
Approach (3)	300	191	0.9929	1.0071	−0.01
"σ_w"	500	41	0.9985	1.0042	0.27
	700	15	0.9995	1.0030	0.25

The mass density used for the dry particles affects both the water activity and the surface tension modelled for a given droplet size. Varying the density of sodium laurate particles over the range 900–1100 kg m^{-3} changed predicted critical supersaturations by up to 5.4% as seen in Table 4.

Solid mass densities of the normal fatty acids decrease systematically with carbon chain length from C8 to C14 (CRC, 2004–2005). If dry particle densities of the corresponding sodium salts decrease in the same order, it could contribute to explain the trend in the agreement between the experimental data and

Table 4. Sensitivity analysis (partitioning model, approach 1)

Parameter	Base value	Perturbation	$SS_c(\%)$ $D_p = 40$ nm	Relative change[a]	$SS_c(\%)$ $D_p = 100$ nm	Relative change[a]
Sodium laurate						
Experimental value			1.24 ± 0.07 [e]		0.35 ± 0.02	
Base case (model)	Approach (1) 'partitioning'	–	1.16	–	0.30	–
σ	Szyskowski equation, σ from Campbell (1965)	Szyskowski equation, σ from Kralchevsky (2007)[b]	1.11	−4.5%	0.28	−5.7%
		eq. (4), σ from Campbell (1965)[c]	1.21	3.9%	0.31	3.5%
		eq. (4), σ from Kralchevsky (2007)[d]	1.15	−0.7%	0.29	−2.1%
ρ	1000 kg m^{-3}	900 kg m^{-3}	1.22	5.4%	0.31	5.3%
		1100 kg m^{-3}	1.11	−4.7%	0.28	−4.6%
T	296.15 K	293.15 K	1.19	2.2%	0.30	2.3%
		299.15 K	1.14	−2.2%	0.29	−2.2%
γ_w, γ_o	1	Debye–Hückel limiting law	1.17	1.2%	0.30	1.1%
γ_w	1	Fineman (1948)	1.16	<−0.1%	0.30	−0.1%
ν_o	2	1.9	1.19	2.6%	0.30	2.5%
		1.95	1.18	1.3%	0.30	1.2%
Sodium caprylate						
Experimental value			0.96 ± 0.05 [e]		0.27 ± 0.02	
Base case (model)	Approach (1) 'partitioning'	–	1.06	–	0.26	–
n_w	$(V_{droplet} - V_{particle})/{\nu_w}^0$	$(\rho_{solution} V_{droplet} - \rho V_{particle})/M_w$, $\rho_{solution}$ from Gonzalez-Perez (2004)	1.06	0.1%	0.26	<0.1%

[a]The relative change is calculated as $(SS_{c,perturbed} - SS_{c,base})/SS_{c,base}$ for the modelled results.
[b]The parameters of eq. (3) were: $a = 1.378 \times 10^{-4}$ N m^{-1} K^{-1}, $b = 2.502 \times 10^{6}$, ${x_o}^{cmc} = 4.000 \times 10^{-6}$.
[c]The parameters of eq. (4) were: $a = 8.156 \times 10^{-4}$ N m^{-1}, $b = 1.996 \times 10^{-3}$ N m^{-1} K^{-1}, $c = 2.650 \times 10^{-5}$ mol m^{-2}, $d = 2.077 \times 10^{-4}$, $e = 2.150 \times 10^{-3}$ mol m^{-2}, $f = 1.371$, ${x_o}^{cmc} = 4.175 \times 10^{-4}$.
[d]The parameters of eq. (4) were: $a = 4.181 \times 10^{-3}$ N m^{-1}, $b = 1.899 \times 10^{-3}$ N m^{-1} K^{-1}, $c = 2.261 \times 10^{-5}$ mol m^{-2}, $d = 1.433 \times 10^{-6}$, $e = -7.070 \times 10^{-3}$ mol m^{-2}, $f = 9.747$, ${x_o}^{cmc} = 4.000 \times 10^{-6}$.
[e]Average of two measurements. Confidence intervals include extremes of confidence intervals from the individual determinations.

modelling approach (1): for sodium caprylate, critical supersaturations predicted by modelling approach (1) are slightly higher than the experimental values, but the differences decrease for increasing carbon chain length and for sodium myristate, the modelled critical supersaturations are lower than the experimental.

This underlines the need for reliable methods of determining densities of atmospheric aerosol particles.

To the best of our knowledge, experimental data on aqueous solution densities are only available for solutions of sodium caprylate. Therefore, the sensitivity analysis related to the partial molar volume of water in the droplet solution was performed for sodium caprylate particles.

The partial molar volume of water in the growing aqueous solution droplets was approximated by the partial molar volume of pure water. To test this assumption, the density ($\rho_{solution}$) of the droplet solution formed on sodium caprylate particles was parameterized as a function of sodium caprylate bulk concentration from experimental data on aqueous sodium caprylate bulk solutions (Gonzalez-Perez et al., 2004). The mass of water in the droplet was determined as the difference between the droplet solution mass, given by the droplet volume and the concentration dependent solution density obtained from the parameterization, and the mass of organic surfactant in the droplet, determined from the dry particle volume and pure surfactant mass density ($m_w^T = \rho_{solution} V_{droplet} - \rho V_{particle}$). From this, the total water number concentration in the droplet solution was calculated using the water molar mass ($n_w^T = m_w^T / M_w$). The organic surfactant total number concentration was determined in the usual way. Calculated critical supersaturations were very close to those obtained using the molar volume of pure water for the partial molar volume of water in the droplet solutions, corresponding to the ideal approximation of zero excess volume of mixing. This is likely because the droplet solutions are so dilute at activation that they indeed behave ideally in having zero excess volumes of mixing.

Temperature enters the Köhler equation in the Kelvin term both directly and indirectly because the calculated surface tension is affected by changes in temperature, see eq. (3). Model calculations of critical supersaturations for all fatty acid salts were

performed at 296.15 K. To investigate the effect of the variation in temperature over the course of the experiments, model calculations for sodium laurate particles were made with temperature variations of ±3 K from the base value. This had only a small effect (<2.5%) on the predicted critical supersaturations.

The droplet bulk concentrations of surfactants have been explicitly evaluated at droplet activation and are so dilute (<0.1M for approach 1 and <0.5 M for approach 3, all dry particle sizes and compositions considered) that both full dissociation of the fatty acid sodium salts and solution ideality appear to be appropriate assumptions. To test the validity of assuming ideality of the solutions, concentration-dependent water activity coefficient parameterizations for sodium laurate solutions were obtained in two ways. First, sodium and laurate mean ionic and water activity coefficients were estimated from the Debye-Hückel limiting law (Robinson and Stokes, 2002). Secondly, molal osmotic coefficients (Φ) for sodium laurate aqueous bulk solutions reported by Fineman and McBain (1948) were converted to water activities as follows (Hamer and Wu, 1972):

$$a_w = \gamma_w x_w = \exp\left(-\Phi \nu_o m_o M_w / 1000\ \mathrm{g\,kg^{-1}}\right), \quad (5)$$

where m_o (mol kg^{-1}) is the organic solute molality. From the water mole fractions in the droplet, water activity coefficients were then calculated. The reported osmotic behaviour for aqueous sodium laurate solutions changes abruptly at the surfactant critical micelle concentration. Therefore, the calculated water activity coefficients were fitted to separate lines for solutions above and below the cmc. The model predicted critical supersaturations for sodium laurate particles were not very sensitive to application of concentration-dependent water activity coefficients for the droplet solutions. This is likely again an indication of dilute droplet solutions at the point of activation.

The sensitivity of model calculations to incomplete dissociation of the fatty acid sodium salts in the droplet bulk was tested by applying dissociation factors of 1.9 and 1.95 to sodium laurate droplet solutions, corresponding to 10 and 5% of the organic salt remaining undissociated in solution. Such variations in the dissociation factor have minor influence (<2.7%) on the model predicted critical supersaturations, see Table 4.

5.2. *Sodium myristate*

Sodium myristate particles activated in the experiments at somewhat higher critical supersaturations than predicted from the partitioning model (approach 1). A possible explanation is that the water activity for droplets above the cmc or solubility limit is not properly evaluated within the model. This could make the first maximum in the Köhler curve higher than currently predicted and possibly dominating. Sodium myristate has the lowest cmc and water solubility of the studied fatty acid sodium salts. As these values are thus more likely to be exceeded in droplets formed on sodium myristate particles, the model treatment above the cmc and solubility limit may therefore be more decisive for sodium myristate than for the other fatty acid sodium salts. The small numerical values of these parameters will also make model calculations for sodium myristate more sensitive to uncertainties herein. Other potential explanations for the poorer agreement between experimental and model calculated critical supersaturations observed for sodium myristate compared to the other fatty acid sodium salts studied are discussed below.

Sodium myristate is the most difficult to properly constrain of the four fatty acid sodium salts studied: very different values have been reported for both the cmc and the equilibrium surface tension at different bulk concentrations of sodium myristate solutions (Campbell and Lakshminarayanan, 1965; Wen et al., 1998; Fainerman et al., 2002; Kralchevsky et al., 2007). The differences between individual literature values are significantly greater than for the other fatty acid sodium salts studied herein. Furthermore, other properties of sodium myristate aqueous solutions such as the formation of myristic acid by myristate protonation, formation of acid-soap complexes and other aggregates, the degree of sodium counterion reassociation to such structures and the precipitation of these much less soluble species remain to be fully quantified (Wen et al., 1998; Wen and Franses, 2000; Wen et al., 2000; Kralchevsky et al., 2007). These effects could lead to a decreased water activity reduction by the solute and thus a higher critical supersaturation compared to the current model results.

Incidentally, assuming no dissociation of sodium myristate in the bulk ($\nu_o = 1$) gives very good agreement between the critical supersaturations predicted by modelling approach (1) and experimental values. This observation may mask one of the effects mentioned above.

Sodium myristate particles were dried to relative humidities in the range 4.5–47% (see Table 2) and we have assumed that the dried particles did not contain residual water. The consistency of the set of measured critical supersaturations observed in Fig. 4d suggests that all particles were of the same phase independently of relative humidity before the CCN-counter. We cannot rule out that the particles have still remained liquid despite of careful drying as discussed, for example, by Hori et al. (2003).

Finally, assuming that the particles produced were indeed solid in the experiments, it is possible that small amounts of soluble impurities in the particles may have lowered the critical supersaturation as explained by Bilde and Svenningsson (2004). Test calculations show that critical supersaturations of sodium myristate are significantly lowered by small amounts of soluble material and that the experimental data can be explained by a few per cent of fully soluble impurity. Similarly, small amounts of impurities can explain the activation behaviour of sodium laurate as fully soluble despite its somewhat limited water solubility observed when preparing solutions for the experiments.

Fatty acid salts with 14, 16, and 18 carbon atoms are the most abundant fatty acid salts in atmospheric aerosols (Gagosian

et al., 1987; Gogou et al., 1994). The properties of sodium myristate which complicates the understanding of the microphysics of cloud droplet activation may also be important for the longer carbon chain fatty acid salts. Our results suggest that the properties of sodium myristate and other longer carbon chain fatty acid salts need to be investigated further within the context of cloud droplet activation.

6. Conclusion

The four fatty acid sodium salts sodium caprylate ($CH_3(CH_2)_6COONa$), sodium caprate ($CH_3(CH_2)_8COONa$), sodium laurate ($CH_3(CH_2)_{10}COONa$) and sodium myristate ($CH_3(CH_2)_{12}COONa$) represent a homologous series of organic surfactants often identified in marine aerosol particles. Our experimental data on dried single-component particles in the size range 33–140 nm show that these fatty acid sodium salts activate to cloud droplets at supersaturations in the range 0.21–1.53%. The supersaturation needed to activate a particle of a given size increases with the carbon chain length. Experimental critical supersaturations for sodium caprylate, caprate and laurate particles were well reproduced by Köhler theory modified to account for surfactant partitioning following the approach of Sorjamaa et al. (2004) assuming full water solubility and full dissociation.

Sodium myristate particles activated at critical supersaturations which were somewhat higher than predicted by the partitioning model with these assumptions. The difference between experimental data and model predictions may be explained by inability within the present model framework to correctly calculate water activities for droplets above the cmc or solubility limit or by solution properties of sodium myristate that act to decrease the water activity reduction by the solute (Raoult effect) from the model-predicted value. The large discrepancies between literature surface tension data for aqueous sodium myristate solutions support the presence of complex solution properties. Consistent with the conclusions of Sorjamaa et al. (2004), Kokkola et al. (2006) and Sorjamaa and Laaksonen (2006), this work confirms that partitioning theory predicts cloud droplet activation of particles containing surface active molecules well. Traditional Köhler theory using the surface tension of pure water also reproduced the experimental critical supersaturations well. This is a balance of overpredicting the water activity reduction (Raoult effect) and omitting the surface tension reduction in the Kelvin effect. The method of using the surface tension of pure water can, however, lead to an erroneous value of the droplet diameter at activation. This deserves further investigation, in particular for more complex, multicomponent aerosol particles. The most important result of this work is that in all cases it was found that Köhler theory using reduced surface tension but not accounting for surfactant partitioning greatly underestimated the observed critical supersaturations.

7. Acknowledgments

We gratefully acknowledge the Nordic Center of Excellence, Research Unit BACCI, the Danish Natural Science Research Council (Copenhagen Center for Atmospheric Research) and the Maj and Tor Nessling Foundation (Grant 2007083) for financial support.

References

Bilde, M. and Svenningsson, B. 2004. CCN activation of slightly soluble organics: the importance of small amounts of inorganic salt and particle phase. *Tellus* **56B**, 128–134.

Blanchard, D. C. 1964. Sea-to-air transport of surface active material. *Science* **146**, 396–397.

Broekhuizen, K., Kumar, P. P. and Abbatt, J. P. D. 2004. Partially soluble organics as cloud condensation nuclei: Role of trace soluble and surface active species. *Geophy. Res. Lett.* **31**, L01107, doi:10.1029/2003GL018203.

Campbell, A. N. and Lakshminarayanan, G. R. 1965. Conductances and surface tensions of aqueous solutions of sodium decanoate, sodium laurate, and sodium myristate, at 25 °C and 35 °C. *Can. J. Chem.* **43**, 1729–1737.

Cheng, Y., Li, S.-M., Leithead, A., Brickell, P. C. and Leaitch, W. R. 2004. Characterizations of cis-pinonic acid and n-fatty acids on fine aerosols in the Lower Fraser Valley during Pacific 2001 Air Quality Study. *Atmos. Environ.* **38**, 5789–5800.

Coltharp, K. A. and Franses, E. I. 1996. Equilibrium and dynamic surface tension behavior of aqueous soaps: Sodium octanoate and sodium dodecanoate (sodium laurate). *Colloids and Surfaces A: Physicochem. Eng. Aspects* **108**, 225–242.

CRC 2004–2005. *Handbook of Chemistry and Physics*. 85th edition. CRC Press, New York.

Delene, D. J. and Deshler, T. 2000. Calibration of a photometric cloud condensation nucleus counter designed for deployment on a balloon package. *J. Atmos. Ocean. Technol.* **17**, 459–467.

Emmenegger, C., Reinhardt, A., Hueglin, C., Zenobi, R. and Kalberer, M. 2007. Evaporative light scattering: A novel detection method for the quantitative analysis of humic-like substances in aerosols. *Environ. Sci. Technol.* **41**, 2473–2478.

Facchini, M. C., Decesari, S., Mircea, M., Fuzzi, S. and Loglio, G. 2000. Surface tension of atmospheric wet aerosol and cloud/fog droplets in relation to their organic carbon content and chemical composition. *Atmos. Environ.* **34**, 4853–4857.

Fainerman, V. B., Miller, R. and Mohwald, H. 2002. General relationships of the adsorption behavior of surfactants at the water/air interface. *J. Phys. Chem. B* **106**, 809–819.

Fineman, M. N. and McBain, J. W. 1948. The osmotic behavior of some colloidal electrolytes as determined by means of the hill-baldes vapor-tension apparatus. *J. Phys. Colloid Chem.* **52**, 881–896.

Gagosian, R. B., Peltzer, E. T. and Zafiriou, O. C. 1981. Atmospheric transport of continentally derived lipids to the tropical North Pacific. *Nature* **291**, 312–315.

Gagosian, R. B., Peltzer, E. T. and Merrill, J. T. 1987. Long-range transport of terrestrially derived lipids in Aerosols from the South-Pacific. *Nature* **325**, 800–804.

Gibbs, J. W., Bumstead, H. A., Longley, W. R. and Van Name, R. G. 1928. *The Collected Works of J. Willard Gibbs*. Longmans, Green and Co., *New York*.

Gill, P. S., Graedel, T. E. and Weschler, C. J. 1983. Organic films on atmospheric aerosol-particles, fog droplets, cloud droplets, raindrops, and snowflakes. *Rev. Geophys.* **21**, 903–920.

Gogou, A., Stephanou, E. G., Stratigakis, N., Grimalt, J. O., Simo, R. and co-authors. 1994. Differences in lipid and organic salt constituents of aerosols from eastern and western mediterranean coastal cities. *Atmos. Environ.* **28**, 1301–1310.

Gonzalez-Perez, A., Ruso, J. M., Prieto, G. and Sarmiento, F. 2004. Apparent molar quantities of sodium octanoate in aqueous solutions. *Colloid Polym. Sci.* **282**, 1133–1139.

Graham, B., Guyon, P., Taylor, P. E., Artaxo, P., Maenhaut, W. and co-authors. 2003. Organic compounds present in the natural Amazonian aerosol: Characterization by gas chromatography-mass spectrometry. *J. Geophys. Res.* **108**(D24), 4766, doi:10.1029/2003JD003990.

Hamer, W. J. and Wu, Y.-C., W. 1972. Osmotic coefficients and mean activity coefficients of uni-univalent electrolytes in water at 25 °C. *J. Phys. Chem. Ref. Data* **1**, 1047–1099.

Henning, S., Rosenorn, T., D'Anna, B., Gola, A. A., Svenningsson, B. and co-authors. 2005. Cloud droplet activation and surface tension of mixtures of slightly soluble organics and inorganic salt. *Atmos. Chem. Phys.* **5**, 575–582.

Hori, M., Ohta, S., Murao, N. and Yamagata, S. 2003. Activation capability of water soluble organic substances as CCN. *J. Aerosol Sci.* **34**, 419–448.

Hyvärinen, A. R., Lihavainen, H., Gaman, A., Vairila, L., Ojala, H. and co-authors. 2006. Surface tensions and densities of oxalic, malonic, succinic, maleic, malic, and cis-pinonic acids. *J. Chem. Eng. Data* **51**, 255–260.

IPCC 2007. *Climate Change 2007—The Physical Science Basis: Contribution of Working Group I to the Fourth Assessment Report of the IPCC*. Cambridge University Press, UK.

Kertes, A. S., Tsimering, L. and Garti, N. 1985. Enthalpies of Solution in Sodium Octanoate + Water +Alcohol Mixtures. *Colloid Polym. Sci.* **263**, 67–74.

Kiss, G., Tombácz, E., Varga, B., Alsberg, T. and Persson, L. 2003. Estimation of the average molecular weight of humic-like substances isolated from fine atmospheric aerosol. *Atmos. Environ.* **37**, 3783–3794.

Kiss, G., Tombácz, E. and Hansson, H.-C. 2005. Surface tension effects of humic-like substances in the aqueous extract of tropospheic fine aerosol. *J. Atmos. Chem.* **50**, 279–294.

Köhler, H. 1936. The nucleus in and the growth of hygroscopic droplets. *Trans. Faraday Soc.* **32**, 1152–1161.

Kokkola, H., Sorjamaa, R., Peräniemi, A., Raatikainen, T. and Laaksonen, A. 2006. Cloud formation of particles containing humic-like substances. *Geophys. Res. Lett.* **33**, L10816, doi:10.1029/2006GL026107.

Kralchevsky, P. A., Danov, K. D., Pishmanova, C. I., Kralchevska, S. D., Christov, N. C. and co-authors. 2007. Effect of the precipitation of neutral-soap, acid-soap, and alkanoic acid crystallites on the bulk pH and surface tension of soap solutions. *Langmuir* **23**, 3538–3553.

Kulmala, M., Laaksonen, A., Charlson, R. J. and Korhonen, P. 1997. Clouds without supersaturation. *Nature* **388**, 336–337.

Laaksonen, A., Korhonen, P., Kulmala, M. and Charlson, R. J. 1998. Modification of the Köhler equation to include soluble trace gases and slightly soluble substances. *J. Atmos. Sci.* **55**, 853–862.

Latif, M. T. and Brimblecombe, P. 2004. Surfactants in Atmospheric Aerosols. *Environ. Sci. Technol.* **38**, 6501–6506.

Li, Y. C. and Yu, J. Z. 2005. Simultaneous determination of mono- and dicarboxylic acids, omega-oxo-carboxylic acids, midchain ketocarboxylic acids, and aldehydes in atmospheric aerosol samples. *Environ. Sci. Technol.* **39**, 7616–7624.

Li, Z. D., Williams, A. L. and Rood, M. J. 1998. Influence of soluble surfactant properties on the activation of aerosol particles containing inorganic solute. *J. Atmos. Sci.* **55**, 1859–1866.

Low, D. H. 1969. A Theoretical Study of Nineteen Condensation Nuclei. *Journal de Recherches Atmospheriques* **4**, 65–78.

Luepakdeesakoon, B., Saiwan, C. and Scamehorn, J. F. 2006. Contact angle of surfactant solutions on precipitated surfactant surfaces. III. Effects of subsaturated anionic and nonionic surfactants and NaCl. *J. Surfact. Deter.* **9**, 125–136.

Mochida, M., Kitamori, Y., Kawamura, K., Nojiri, Y. and Suzuki, K. 2002. Fatty acids in the marine atmosphere: Factors governing their concentrations and evaluation of organic films on sea-salt particles. *J. Geophys. Res.* **107**(D17), 4325, doi:10.1029/2001JD001278.

Mochida, M., Kawabata, A., Kawamura, K., Hatsushika, H. and Yamazaki, K. 2003a. Seasonal variation and origins of dicarboxylic acids in the marine atmosphere over the western North Pacific. *J. Geophys. Res.* **108**(D6), 4193, doi:10.1029/2002JD002355.

Mochida, M., Kawamura, K., Umemoto, N., Kobayashi, M., Matsunaga, S. and co-authors. 2003b. Spatial distributions of oxygenated organic compounds (dicarboxylic acids, fatty acids, and levoglucosan) in marine aerosols over the western Pacific and off the coast of East Asia: Continental outflow of organic aerosols during the ACE-Asia campaign. *J. Geophys. Res.* **108**(D23), 8638, doi:10.1029/2002JD003249.

Mochida, M., Umemoto, N., Kawamura, K., Lim, H. J. and Turpin, B. J. 2007. Bimodal size distributions of various organic acids and fatty acids in the marine atmosphere: Influence of anthropogenic aerosols, Asian dusts, and sea spray off the coast of East Asia. *J. Geophys. Res.* **112**(D15209), doi:10.1029/2006JD007773.

O'Dowd, C. D., Facchini, M. C., Cavalli, F., Ceburnis, D., Mircea, M. and co-authors. 2004. Biogenically driven organic contribution to marine aerosol. *Nature* **431**, 676–680.

Prisle, N. L. 2006. Cloud Condensation Nuclei Properties of Organic Aerosol Particles: Effects of Acid Dissociation and Surfactant Partitioning, M. Sc. Thesis, Department of Chemistry, University of Copenhagen.

Robinson, R. A. and Stokes, R. H. 2002. *Electrolyte Solutions*. Second Revised Edition. Dover Publications, New York.

Ross, S. and McBain, J. W. 1946. Diffraction of X-rays by sodium oleate and hexanolamine oleate. *J. Am. Chem. Soc.* **68**, 547–550.

Seidl, W. and Hanel, G. 1983. Surface-active substances on rainwater and atmospheric particles. *Pure Appl. Geophys.* **121**, 1077–1093.

Shelley, M. Y., Sprik, M. and Shelley, J. C. 2000. Pattern formation in a self-assembled soap monolayer on the surface of water: A computer simulation study. *Langmuir* **16**, 626–630.

Shulman, M. L., Jacobson, M. C., Carlson, R. J., Synovec, R. E. and Young, T. E. 1996. Dissolution behavior and surface tension effects of organic compounds in nucleating cloud droplets. *Geophys. Res. Lett.* **23**, 277–280.

Snider, J. R., Petters, M. D., Wechsler, P. and Liu, P. S. K. 2006. Supersaturation in the Wyoming CCN instrument. *J. Atmos. Ocean. Technol.* **23**, 1323–1339.

Sorjamaa, R., Svenningsson, B., Raatikainen, T., Henning, S., Bilde, M. and co-authors. 2004. The role of surfactants in Köhler theory reconsidered. *Atmos. Chem. Phys.* **4**, 2107–2117.

Sorjamaa, R. and Laaksonen, A. 2006. The influence of surfactant properties on critical supersaturations of cloud condensation nuclei. *J. Aerosol Sci.* **37**, 1730–1736.

Stahl, P. H. and Wermuth, C. G. 2002. *Handbook of Pharmaceutical Salts, Properties, Selection and Use*. Wiley-VCH and Verlag Helvetica Chimica Acta, Switzerland.

Stephanou, E. G. 1992. Biogenic and anthropogenic organic compounds in eolian particulates in the east mediterranean region-I. occurrence and origin. *Atmos. Environ. Part A: General Topics* **26**, 2821–2829.

Szyskowski, B. V. 1908. Experimentelle studien über kapillare eigenschaften der wässerigen lösungen von fettsauren. *Zeitschrift für Physikalische Chemie* **64**, 385–414.

Tabazadeh, A. 2005. Organic aggregate formation in aerosols and its impact on the physicochemical properties of atmospheric particles. *Atmos. Environ.* **39**, 5472–5480.

Taraniuk, I., Graber, E. R., Kostinski, A. and Rudich, Y. 2007. Surfactant properties of atmospheric and model humic-like substances (HULIS). *Geophys. Res. Lett.* **34**, L-16807, doi:10.1029/2007GL029576.

Van Den Bogaert, R. and Joos, P. 1979. Dynamic surface tensions of sodium myristate solutions. *J. Phys. Chem.* **83**, 2244–2248.

Van Den Bogaert, R. and Joos, P. 1980. Diffusion-controlled adsorption-kinetics for a mixture of surface-active agents at the solution-air interface. *J. Phys. Chem.* **84**, 190–194.

Van Egmond, R., Hambling, S. and Marshall, S. 1999. Bioconcentration, biotransformation, and chronic toxicity of sodium laurate to zebrafish (Danio rerio). *Environ. Toxicol. Chem.* **18**, 466–473.

Wen, X. Y., McGinnis, K. C. and Franses, E. I. 1998. Unusually low dynamic surface tensions of aqueous solutions of sodium myristate. *Colloids and Surfaces A: Physicochem. Eng. Aspects* **143**, 371–380.

Wen, X. Y. and Franses, E. I. 2000. Effect of protonation on the solution and phase behavior of aqueous sodium myristate. *J. Colloid Interface Sci.* **231**, 42–51.

Wen, X. Y., Lauterbach, J. and Franses, E. I. 2000. Surface densities of adsorbed layers of aqueous sodium myristate inferred from surface tension and infrared reflection absorption spectroscopy. *Langmuir* **16**, 6987–6994.

Yassaa, N., Meklati, B. Y., Cecinato, A. and Marino, F. 2001. Particulate n-alkanes, n-alkanoic acids and polycyclic aromatic hydrocarbons in the atmosphere of Algiers City Area. *Atmos. Environ.* **35**, 1843–1851.

Yassaa, N. and Cecinato, A. 2005. Composition of torched crude oil organic particulate emitted by refinery and its similarity to atmospheric aerosol in the surrounding area. *Chemosphere* **60**, 1660–1666.